Using combined slots as a new approach for optimizing erodible bed changes around the spur dikes in series

Mehran Kheirkhahan, Shahab Nayyer, Khosrow Hosseini & Sayed-Farhad Mousavi

Published online: 16 Dec 2022.

Submit your article to this journal ⧉

View related articles ⧉

View Crossmark data ⧉

Check for updates

Using combined slots as a new approach for optimizing erodible bed changes around the spur dikes in series

Mehran Kheirkhahan, Shahab Nayyer, Khosrow Hosseini and Sayed-Farhad Mousavi

Department of Water Engineering and Hydraulic Structures, Faculty of Civil Engineering, Semnan University, Semnan, Iran

ABSTRACT

The common spur dikes, which are used for river path control and bank protection, are utilized without any slots or with additional structures such as a collar or vane. The present research has been conducted to optimize the slot position in the spur dikes' body, reduce the scour depth, and improve the sedimentation conditions using the *CFD* model. The numerical result was compared with the Nayyer et al. 2019. A numerical and experimental investigation of the effects of combination of spur dikes in series on a flow field. *Journal of the Brazilian Society of Mechanical Sciences and Engineering*, *41*(6), 1–11) experimental outcome. Results showed that the (L_{S-W-Wi}, T_{S-W}, T_{S-W-Wi}) combination contained the slots in the web and wing of the first and third spur dike, and the slot at the web of the middle spur dike was found as the best combination of slots under clear-water conditions. This combination was conducted to reduce the scour depth by 6.8% and increase deposition by 52% compared to the spur dikes without slots, which causes reducing scour depth and an increase in the sedimentation rate of materials between two consecutive spur dikes in series. Also, the maximum scours depth decreases by up to 20%. The results revealed that the presence of slots in spur dike and their different positions have complicated and considerable influences on the form and morphology of the bed.

1. Introduction

Bank erosion and bed changes in rivers have always been of interest to engineers. Various methods and structures exist, such as spur dikes to control bank erosion and bed river changes. Spur dikes could be implemented with Simple, *L*–shaped, *T*-shaped, triangular, and other forms with different angles concerning the flow direction. Scouring around spur dikes is produced by down-flow and initial vortices at the upstream corner of the spur dike. In addition, secondary eddies and wakes are in the middle and their downstream corner (Barbhuiya & Dey, 2004; Coleman et al., 2003). Therefore, different methods are proposed to reduce scouring and prevent undesirable effects on the stability of the structure, such as changing the flow pattern and decreasing its intensity. The use of collars, vanes, a combination of spur dikes in series, and slots are part of the leading solutions for changing the flow pattern (Chiew, 1992; Nayyer et al., 2019).

Slots reduce the strength of down-flow and horseshoe vortex. Slots induce horizontal flow in the bed's vicinity, which lowers pressure gradients and down-flow transfers away from the structure. All these effects lead to a reduction in scouring around spur dikes (Kumar 1996). Scour depth reduction around bridge piers; using the slots under different conditions has been investigated by various researchers, such as Kumar et al. (1999), Babar et al. (2000), and Tafarojnoruz et al. (2012). In all of these researches, the efficiency of slots is approved, and some research is on the erosion around the spur dikes, which are the most relevant, are reviewed here. Hasanpour et al. (2012) revealed in their study that the slots reduce the scour depth around spur dikes; their reduction has been reported by about 28%. Gu et al. (2016) stated that all turbulence models (*k-ε*, *RNG*, and *LES*) are appropriate for simulating the three-dimensional flow around the spur dike. They recommended the standard *k-ε* turbulence model for main flow field characteristics simulation around the non-submerged spur dike in series.

Dorosti et al. (2018) showed that the slot in the spur dike's body near the bed performed well in balancing sedimentation height and local scouring. Masjedi and Jafari (2018) showed that the minimum scours depth occurred in the slot in the vicinity of the spur dike tip. Also, the scouring is increased by raising the distance between the slot and the spur dike tip. Monjezi et al. (2019) proposed a dimensionless parameter named slot ratio (*x/l*), which described the ratio of the distance between the slot edge and the spur dike tips (*x*) and spur dike length (*l*). When the slot ratio equals 0.25, riprap stability at the bend was more stable than the slot ratio equals 0.75. Nayyer et al. (2019) stated that the (*LTT*) combination of spur dikes had the highest effect on reducing the velocity, shear stress, and turbulence intensity around the spur dikes. So, it seems that a combination of different geometries could considerably reduce the scouring and increase the sedimentation between spur dikes.

Scouring depth around the spur dike, which was installed in the bed with a sand-gravel mixture, was analyzed experimentally by Pandey et al. (2019). Their result showed that the non-dimensional maximum equilibrium scours depth by the effect of critical velocity, Froude number for sediment mixture and water depth increases, and also with an increase in armour particle-spur dike length ratio, decreases. The other research by Pandey et al. (2021) concluded that by increasing the threshold velocity ratio, the Froude number, and the flow depth-particle size ratio, scour depth grows around a vertical spur dike. Vaghefi et al. (2021) investigated

the effect of a *T*-shaped spur dike on the downstream bridge pier at a 180-degrees bend. They reported that the spur dike located at the 70-degrees of the outer bend significantly reduces the scour depth around the bridge pier by up to 50 percent. Emamgholizadeh et al. (2021) reported that the Simple, *T*, and *L*-shaped single spur dike could reduce 80, 93, and 96 percent of the scour depth around the bridge abutment, which is located downstream, respectively.

The flow field in the vicinity of the permeable spur dike was investigated by Iqbal et al. (2021) in a rectangular channel. They suggested that a permeable spur dike reduced the turbulent intensity and the field's recirculation region during floods compared to a non-permeable spur dike. Tripathi and Pandey (2021), Akbari et al. (2021), Kafle (2021), and Athar and Nishank Aggarwal (2021) investigated the scour around the Simple and *T*-shaped spur dike and reported the maximum scouring condition in their research. Özyaman et al. (2022) concluded that in all the experimental results, the scour depth around a single spur dike for uniform sediments is more profound than that for non-uniform sediments.

Flow field around permeable spur dike with different staggered pores was investigated by Haider et al. (2022) for different angles. They used (*ANSYS Fluent*) numerical model for their simulation. Their results showed that turbulence and flow field improved using permeable spur dikes (0°) compared to impermeable spur dikes.

In this research, after verification tests of the numerical model, the position of a combination of slots in the body of spur dikes will be analyzed, and the changes in the bed around them will be investigated using a numerical model. Indeed, our research novelty, which deserves attention, is the optimum combinational slot position on the spur dike's body and the reduction of scouring without using any additional structures.

2. Materials and methods

2.1. Experimental model

Verification tests are usually proposed to validate the numerical models. For this purpose, Nayyer et al. (2019) experimental model and setup were used. They used a rectangular flume 14 m long, 1.5 m wide, and 0.6 m height in which the bed is covered with a layer of uniform gravel sediment with $D_{50} = 1$ mm and a geometric standard deviation of 1.41.

In their experiment, the flow rate (Q), and flow depth (y) were 28.5 *lit/s* and 6 cm for clear-water conditions, respectively. Also, the geometric characteristics of the used spur dikes in the research by Nayyer et al. (2019) are shown in Figure 1, in which $a = 3L$, $L = L_t$, and $L/B = 0.23$. According to their result, the optimum combination of spur dikes (*LTT* series) is used for simulation and investigation of creating slots in the web and wing of the spur dikes in the numerical model.

2.2. Numerical model

2.2.1. Numerical model and the governing equations
Software such as Flow-3D was developed to model different phenomena. This software profits some special techniques which permit the model of various physical and numerical conditions for real or experimental models. The general forms of mass and momentum conservation equations in the *CFD* model are given by Equation (1) and Equation (2), respectively:

$$V_F \partial\rho/\partial t + \partial/\partial x(\rho u A_x) + \partial/\partial y(\rho v A_y) + \partial/\partial z(\rho w A_z) = 0 \tag{1}$$

$$\partial u/\partial t + 1/V_F\{uA_x(\partial u/\partial x) + vA_y(\partial u/\partial y) + wA_z(\partial u/\partial z)\} = (-1/\rho)(\partial p/\partial x) + G_x + f_x - b_x \tag{2a}$$

$$\partial v/\partial t + 1/V_F\{uA_x(\partial v/\partial x) + vA_y(\partial v/\partial y) + wA_z(\partial v/\partial z)\} = (-1/\rho)(\partial p/\partial y) + G_y + f_y - b_y \tag{2b}$$

$$\partial w/\partial t + 1/V_F\{uA_x(\partial w/\partial x) + vA_y(\partial w/\partial y) + wA_z(\partial w/\partial z)\} = (-1/\rho)(\partial p/\partial z) + G_z + f_z - b_z \tag{2c}$$

Where *u, v, w*, are velocity components and A_x, A_y and A_z are the fractional area open to flow, respectively, in *x, y,* and *z* directions, V_F is the fractional volume open to flow, ρ is the fluid density, *G* is body acceleration, *f* is a term of viscous acceleration, and *b* is flow losses in across porous baffle plate or porous media (Flow Science Inc 2008).

In the *CFD* model, the *FAVOR* method is used to model solid surfaces, geometries, and volumes, which helps to achieve the best mesh size. Also, the *VOF* method is used to trace the water surface in a water–air two-phase flow. Expression (3) is proposed for defining the free surface profile.

$$\partial F/\partial t + u_j \partial F/\partial x_j = 0 \tag{3}$$

where *F* function is the index of volume percentage of the water phase in a cell; it ranges between zero) for the case in which the cell is full of air (and one (for the case in which the cell is full of water) (Hirt & Nichols, 1981).

Different methods, such as Meyer Peter and Müller, and Von Rijn, are proposed in the *CFD* model for modelling the bed load. Also, the suspended load is modelled using *ADE* (Advection–diffusion equation) given by expression (4):

$$\partial c/\partial t + U_i(\partial c/\partial x_i) + W_s(\partial c/\partial z) = \partial/\partial x_i(\Gamma(\partial c/\partial x_i)) \tag{4}$$

In this equation, *c* is the sediment concentration, *U* is the average Reynolds velocity of flow, W_s denotes the fall velocity of sediment particles, *x* and *z* represent the dimension along the main direction and vertical direction, respectively. Also, Γ is the coefficient of dispersion defined as the ratio of turbulent viscosity to Schmidt number (Flow Science Inc 2008).

2.2.2. Turbulent models
Studying the characteristics of turbulent flow is very complex and time-consuming. In this flow type, currents with different momentums encounter each other and reduce the fluid kinetic energy. This dissipated energy is converted to heat in a one-way process. All the issues mentioned earlier should be considered when investigating turbulent flow. Therefore, numerical models can present valuable information to solve turbulent problems (Farzin et al., 2018).
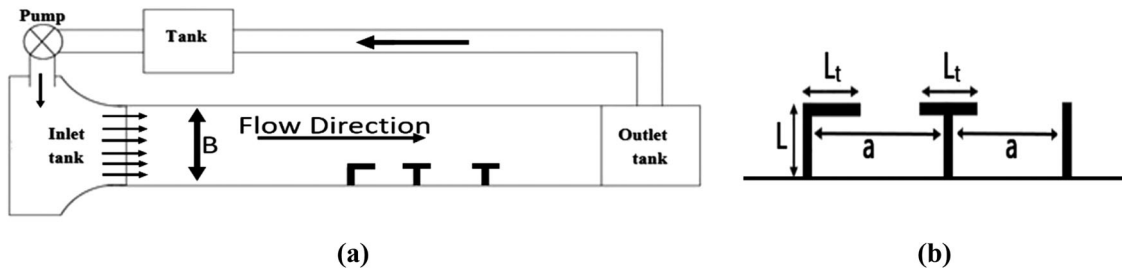
Figure 1. a) Experimental flume and b) geometric parameters of the spur dikes.

The present study defined turbulent models such as k-ε, RNG, and LES in the CFD model used for simulation. According to numerical model validation, the optimum turbulent model will have selected.

2.2.3. Mesh and Boundaries

As stated before, The CFD model was incorporated for the simulation of the experimental model. The boundary condition used for the directions were Wall for the direction of Z_{min}, Y_{max}, and Y_{min}, Symmetry as a free surface for Z_{max}, Volume Flow-Rate for X_{min} as inflow boundary, and Pressure for output boundary (X_{max}). These boundary conditions were selected according to the experimental model and situation of scouring phenomena around the spur dikes, which is illustrated in Figure 2. (d). As mentioned previously, the $FAVOR$ method models solid surfaces, geometries, and volumes which helps to achieve the best mesh size. Modelling was performed in the software using two flow rate values of 28.5 and 25.65 lit/s with 6 cm depth.

2.2.4. Evaluation and comparison criteria

The evaluation and comparison of numerical and experimental values were considered by using three criteria, mean absolute error (MAE) and root mean square error ($RMSE$), and coefficient of determination (R^2) and defined by Equation (5): where O (the experimental values), P (values obtained in the numerical model) and n (total number of data) (Nayyer et al., 2019).

$$R^2 = 1 - \left[\frac{\sum_{i=1}^{n}(O-P)^2}{\sum_{i=1}^{n}O^2 - \left(\frac{\sum_{i=1}^{n}P^2}{n}\right)} \right], RMSE$$

$$= \sqrt{\frac{\sum_{i=1}^{n}(O-P)^2}{n}}, MAE = \frac{1}{n}\sum_{i=1}^{n}|O-P| \quad (5)$$

2.2.5. Slot's dimensions and shapes

As stated before, this research aims to investigate the slot's effect on the scour depth of spur dikes in series. The LTT series of spur dikes was introduced as the optimum combination obtained by Nayyer et al. (2019). Therefore, the slot was defined for this combination. The slot shape was considered as a horizontal rectangle in the body of spur dikes with the ratio of $a_s/b_s = 4$ (a_s is the length, b_s is the width, and t is the thickness of the slot) and the opening area of 10% of the structure effective area (Chiew, 1992). Also, the position of the horizontal slots was taken close to the bed level (Dorosti et al., 2018). Figure 2 shows the defined geometry and position of the slot in the spur dike body.

The intended combinations with the slots in the web and wing of the spur dikes are given in Table 1. In this table, the position of the slot (S) in the web (W) and wing (W_i) are written at the side of each spur dike and its situation.

3. Results and discussion

3.1. A comparison between numerical and experimental results

RNG, k-ε, and LES turbulence models were used to investigate the numerical model and obtain the appropriate result. A Comparison of scour depth for the experimental (Nayyer et al., 2019) and numerical results for the LTT combination concluded that for RNG, k-ε, and LES, the amount of R^2 is equal to 0.97, 0.99, and 0.90, and $RMSE$ is equal to 0.66, 0.12, 1.47, and also MAE is equal to 0.19, 0.03 and 0.43, respectively. So, with the optimum mesh and turbulence model selected according to the comparison between numerical simulation and experimental scour depth, all simulations will be continued with them. Therefore, for the continuation of the simulation, the results of the intended meshing and the k-ε turbulence model showed that the statistical indices values for these models are equal to $R^2 = 0.97$, $RMSE = 0.28$, and $MAE = 0.24$ for erodible bed changes.

A comparison of bed change between the eroded bed in the experimental model by Nayyer et al. (2019) and the numerical model in this research is shown in Figure 3. The results of maximum scour depth for the first, second, and third spur dikes in comparison to the experimental results are shown in Figure 4. As seen, this numerical model has presented acceptable results with good accuracy. The LTT combination of spur dikes in series was modelled for 700 s, and it was observed that after 500 s of simulation, the flow condition fully developed, and the scour depth reached to equilibrium condition, as shown in Figure 5. As is observed in about 30% of simulation duration the scour depth reached 85% of the equilibrium scour depth. Nayyer et al. reported that spur dikes reach more than 90% of equilibrium erosion within 10% of erosion time for the T-shaped series, while the Simple and L-shaped series reaches 80% of equilibrium scour depth within 15% of elapsed time (Nayyer et al., 2018). These differences can be related to the shape of spur dikes used in the series.

3.2. Slot effect on erosion

Due to the complexity associated with investigating the effect of the slot on the bed and changes in the scour depth around the spur dikes, this effect should be investigated in different aspects. Therefore, the maximum scour depth,
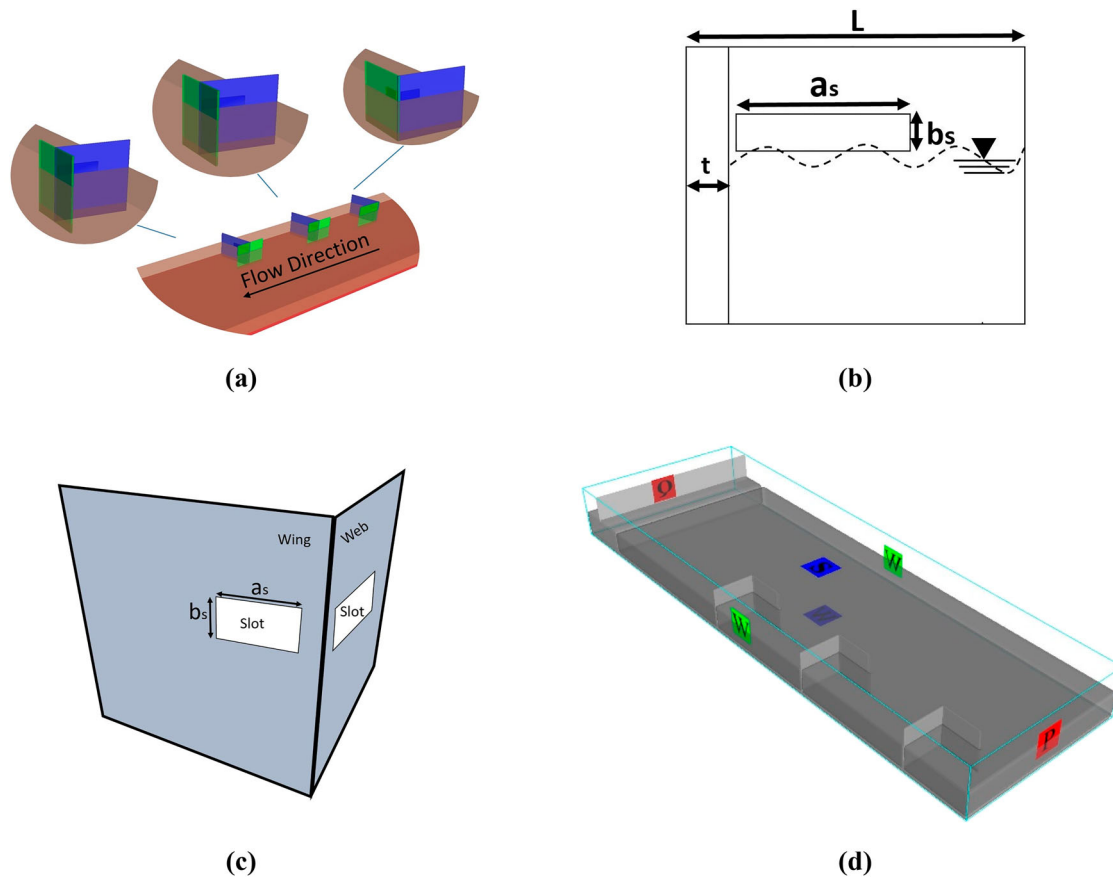
Figure 2. a) geometry of the spur dikes and their slots, b) slot characteristics and position of it in the spur dike web, c) position of the slot in spur dike web and wing in L-shaped spur dike, d) boundary conditions.

sedimentation, and overall erosion of the bed are part of the parameters analyzed in this research.

The first spur dike in all the combinations of Table 1 had the highest scour depth. Therefore, to investigate the effect of the slot in the first spur dike, models 1–8 were simulated to be examined for two different flow rates. Models No. 1 and 5 were without a slot, models 2 and 6 had a slot in the web of the first spur dike, models 3 and 7 had a slot in the wing of the first spur dike, and models 4 and 8 had slots in the web and wing of the first spur dike. The results showed that the scour depth in the first spur dike is reduced in any slot position. Hasanpour et al. (2012) reported the same consequence in their research. The minimum reduction corresponds to models 3 and 7 with the slot in the wing which is about 5% with respect to the state without a slot. The maximum reduction corresponds to models 2 and 6

with a slot on the web which is about 55% with respect to the state without a slot. Models 4 and 8 also have about a 25% reduction in the scour depth at the position of the first spur dike. The noteworthy point in all these models is that although the scour depth is reduced at the position of the first spur dike, it is increased at the positions of the second and third spur dikes.

Therefore, changes in erosion and sedimentation were investigated over the entire bed length till the effect of the slot in the first spur dike was determined along the entire bed length. Figure 6 shows changes in the scour depth and in the ratio of the sedimentation to erosion in models 1–8. As seen in models 2 and 6, the mean scours depth of the spur dikes was reduced, but the ratio of sedimentation to erosion was also reduced. The other point is related to models 2 and 6, where the maximum scour depth has occurred at the position of the second spur dike, which is different from other models.

Models 3 and 7 also illustrate an increase in the mean scour depth at the position of spur dikes due to the rise in the scour depth at the positions of the second and third spur dikes. Also, in these models, the bed sedimentation to erosion ratio was reduced. Finally, in models 4 and 8, the mean scour depth had a significant reduction; on the other hand, the ratio of sedimentation to erosion had a considerable increase. Models 4 and 8, which have slots in the web and wing of the first spur dike, represent acceptable performance in terms of both reductions in the mean scour depth and sedimentation. The mentioned recent result was confirmed by an investigation by Dorosti et al. (2018), which stated that the presence of the slot in the body of the spur dike near the bed conducted good performances

Table 1. Characteristics of the used models in the present study.

Model ID	Discharge (l/s)	First Spur Dike	Second Spur Dike	Third Spur Dike
1	28.5	L	T	T
2	28.5	L_{S-W}	T	T
3	28.5	L_{S-Wi}	T	T
4	28.5	L_{S-W-Wi}	T	T
5	25.65	L	T	T
6	25.65	L_{S-W}	T	T
7	25.65	L_{S-Wi}	T	T
8	25.65	L_{S-W-Wi}	T	T
9	28.5	L_{S-W-Wi}	T_{S-W}	T
10	28.5	L_{S-W-Wi}	T_{S-W}	T_{S-W}
11	28.5	L_{S-W-Wi}	T_{S-W}	T_{S-W-Wi}
12	28.5	L_{S-W-Wi}	T_{S-W-Wi}	T
13	28.5	L_{S-W-Wi}	T_{S-W-Wi}	T_{S-W}
14	28.5	L_{S-W-Wi}	T_{S-W-Wi}	T_{S-W-Wi}

(a) **(b)**
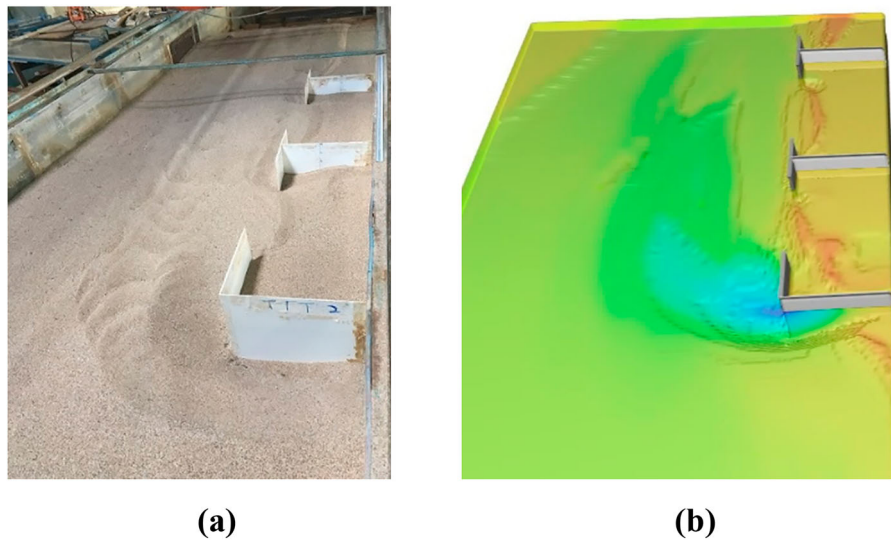
Figure 3. Eroded Bed a) experimental model of Nayyer et al. [4], b) scour depth in the present research numerical model.

in providing the balance between sedimentation height and local scouring. Figure 7 shows the bed level for both of these models.

As stated before, the presence of the slot in the first spur dike, in any case, causes a reduction of scour depth in the first spur dike and an increase of scouring in the second and third spur dikes. Therefore, in models 9–14, the slot in the web and wing of the first spur dike is constant, and the slot in the spur dikes at the second and third positions was investigated. Considering that scouring increases at the second and third spur dikes, that model would yield the best result, which has a minimum rise in the scour depth at the spur dikes of the second and third positions and also the maximum rate of sedimentation and the minimum rate of erosion over the entire bed length.

Table 2 summarizes the obtained results from simulations of models 9–14. As observed, changes in the bed in all the models were associated with increasing sedimentation and reducing erosion of the entire bed length. These results conformed with the research consequence of Chiew (1992), Kumar (1996), Hasanpour et al. (2012), Monjezi et al. (2019), Dorosti et al. (2018), and Masjedi and Jafari (2018), which all of them reported the reducing effect of slot on scouring around spur dike. The maximum sedimentation corresponds to model 11, and the minimum corresponds to model 10. In model 11, the slot was in

the web and wing of the first and third spur dikes, and the second spur dike was defined on the web. Also, in model 10, the slot was created in the web and wing of the first spur dike and the web of the second and third spur dike.

Change in the bed erosion over its entire length is insignificant in all the models, and there is not much difference between them. However, considering the ratio of sedimentation to erosion, it is concluded that the best ratio belongs to model 11. The height of sedimentation concerning the scour depth in model 11 has a higher value, indicating good sedimentation in this model. Also, considering the maximum scour depth, all models 9–14 had been associated with a noticeable reduction in the scour depth at the position of the first spur dike. In addition, in all the cases, the first spur dike had maximum scour depth and no longer performed similarly to models 2 and 6.

The maximum scour depth reduction corresponds to model 12, although model 11 had a considerable reduction. By Considering the sedimentation condition and the decrease in the scour depth, it could be stated that model 11 had acceptable and appropriate performance. The bed elevation and streamlines around the series of spur dikes in models 1 and 11 are shown in Figure 8, with 6 cm of flow depth. As is seen, creating slots in the body of spur dikes
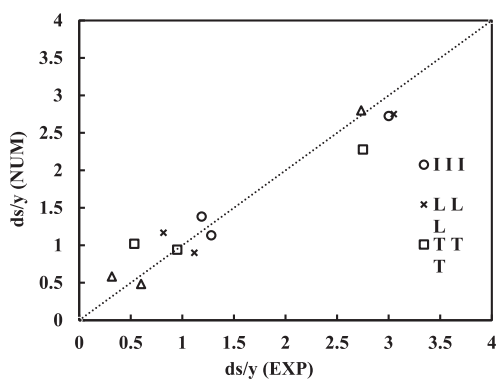
Figure 4. Comparison between the equilibrium scour depth values in the experimental and numerical models.
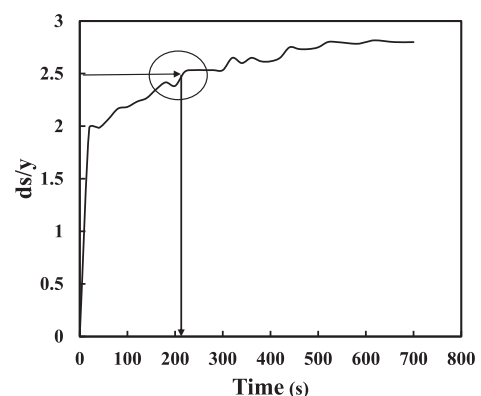
Figure 5. Temporal changes of the scour depth in LTT combination.
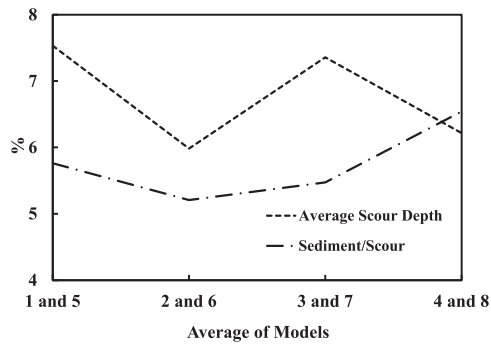
Figure 6. Changes in the mean scour depth and ratio of sedimentation to erosion.

changes the streamlines. In model 1, the vortex flow was formed between the spur dikes (between the first and second spur dikes and between the second and third spur dikes). For a spur dike without a slot, the flow after a collision with the spur dike's body returns its path and forms the vorticities around the structures. But for the spur dike with the slot, some part of the stream can pass through the slots, and some of that return its path, so because of this passing in the body of the spur dike, the intensity of flow is reduced and has a less destructive effect on bed changes. On the other hand, because of the decreases in the carrying capacity of sediment particles of flow passed from slots, the sedimentation occurs more than from the other state.

Also, the diverted streamlines at the position of the first spur dike had greater flow interference due to the high flow diversion at this location. In this model, the inflow between two spur dikes exits the entrance section ultimately. However, in model 11, the conditions are different. The vortex flow between the spur dikes in model 11 is smaller and formed between the spur dike's web and the downstream wall. Two groups of flows enter the field between the two spur dikes; the flows which enter from the slots and those which enter from the section between the two consequent spur dikes. The outflow also forms in slots downstream and the section between the two consequent spur dikes. The other point seen in the streamlines of model 11 is that some flows enter the space between the first and second spur dikes and finally exit from the third spur dike body, whereas in model 1, this type of flow does not exist.

4. Conclusion

The present research novelty that deserves attention is the optimum combinational slot position in the spur dike's body and the reduction of scouring without using any

additional structures. So, in the present research, by employing the *CFD* model, the optimum combination of spur dikes (*LTT*) of Nayyer et al. (2019) was simulated with different slot positions on the body of spur dikes to reduce the scour depth around the spur dikes and improve the sedimentation conditions.

Finally, the effect of combined slots within the web and wing of the optimum spur dikes series was investigated. Moreover, the (L_{S-W-Wi} T_{S-W} T_{S-W-Wi}) combination with slots in the web and wing of the first and third spur dike and also slot in the web of the second spur dike was selected as the best combination for reducing the scour depth and increase of sedimentation. In continuation, the other results are presented.

- The CFD model has successfully simulated and analyzed the flow condition around the spur dike and erodible bed. The statistical indexes values for comparing the experimental and numerical results in models of this research were R2 = 0.97, RMSE = 0.28, and MAE = 0.24.
- Using the slot only in the body of the first spur dike could significantly reduce the maximum scour depth by up to 55%; this is because of the change in the streamline, which passes across the body of the spur dike and reduces the downward stream and eddies. This percentage where the slot was created both in the web and wing of the first spur dike is 25%. Also, the ratio of sedimentation height to the total bed erosion is about 6.5% higher compared to the case where there is no slot.

Table 2. Bed change for models with slots vs. without slots.

Model ID	Sediment (%)	Scour (%)	Sediment/ Scour (%)	Maximum scour depth (%)	Max scour depth location
9	32	−5	6.1	−21	at tip of first spur dike
10	15	−6	5.3	−13	at tip of first spur dike
11	52	−3	6.8	−20	at tip of first spur dike
12	29	−4	5.8	−23	at tip of first spur dike
13	32	−6	6.0	−15	at tip of first spur dike
14	52	−2	6.7	−15	at tip of first spur dike

Model ID: 4   Model ID: 8
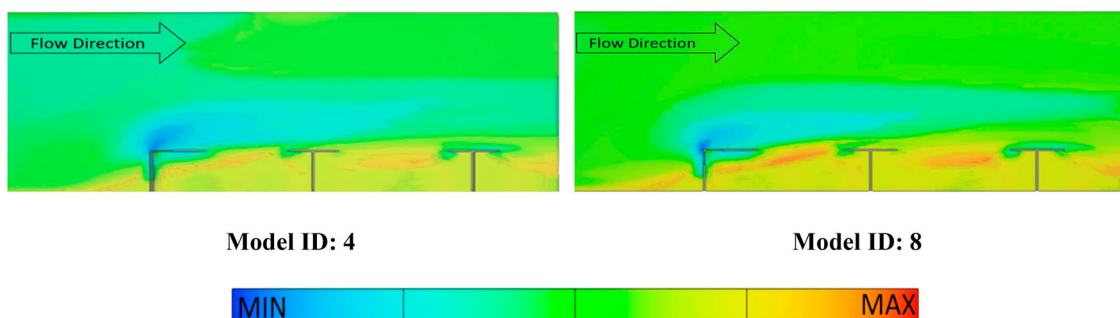
Figure 7. Bed level in models No. 4 and 8.
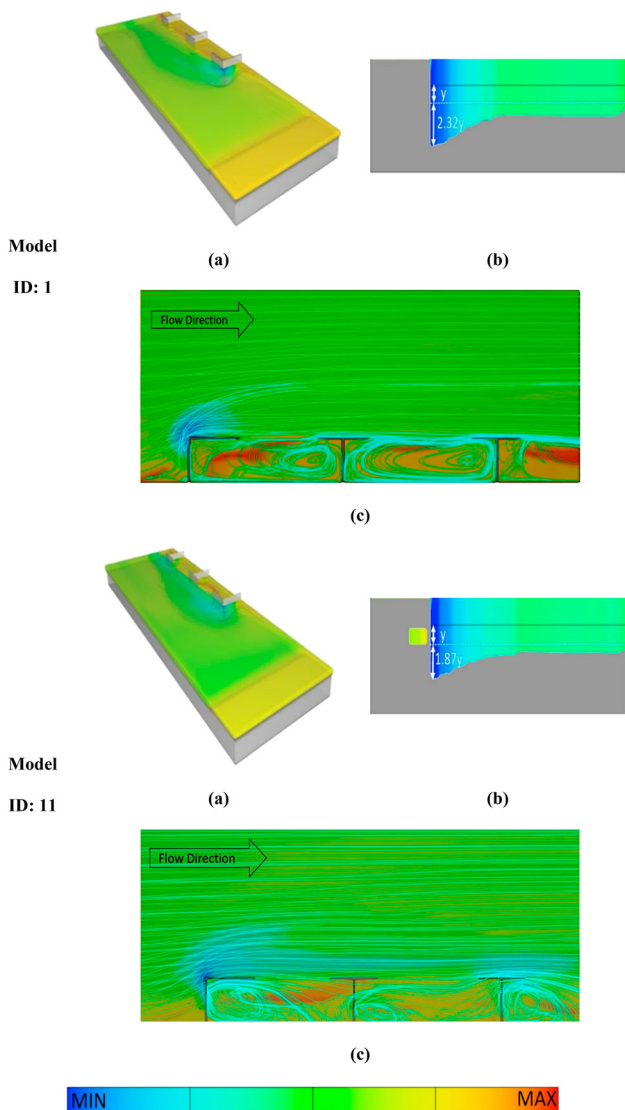
Figure 8. Results of bed change for models No. 1 and 11: a) – 3D view of changes in the bed, b) Cross section at the tip of the first spur dike, c) streamlines.

- The presence of the slot in the body of the second and third spur dikes also causes a reduction in the scour depth under clear-water conditions. In the case where the slot is in the body of the second spur dike and the web and wing of the third spur dike, sedimentation is increased up to 52%, and the ratio of the sedimentation height to the total bed erosion is increased up to 6.8% between two consecutive spur dikes in series. Also, the maximum scour depth reduces by up to 20%.

Finally, the presence of the slot in the spur dike structure and its various positions have a complex and significant effect on the form and morphology of the erodible bed.

For the future, it could be a good idea that the optimum combination of the present research is modeled with the collar, vane, or protective spur dike in different flow field and bed situations.

Authors contributions

All authors contributed to the design and implementation of the research, to the analysis of the results, and to the writing of the manuscript.

Disclosure statement

No potential conflict of interest was reported by the author(s).

References

Akbari, M., Vaghefi, M., & Chiew, Y. M. (2021). Effect of T-shaped spur dike length on mean flow characteristics along a 180-degree sharp bend. *Journal of Hydrology and Hydromechanics*, 69(1), 98–107. doi:10.2478/johh-2020-0045

Athar, M., & Nishank Aggarwal, T. (2021). Effects of spur dyke's orientation on bed variation in channel bend. *Hydro Science and Marine Engineering*, 3(2), 1–9. doi:10.30564/hsme.v3i2.3834

Babar, R., Setia, S., & Setia, B. (2000). Scour protection by a slot through a model bridge pier. *In Proceeding of International Symposium on Recent Advances in Experimental Fluid Mechanics*. Indian Institute of Technology. Kanpur, India.

Barbhuiya, A. K., & Dey, S. (2004). Local scour at abutments: A review. *Sadhana*, 29(5), 449–476. doi:10.1007/BF02703255

Chiew, Y. M. (1992). Scour protection at bridge piers. *Journal of Hydraulic Engineering*, 118(9), 1260–1269. doi:10.1061/(ASCE)0733-9429(1992)118:9(1260)

Coleman, S. E., Lauchlan, C. S., & Melville, B. W. (2003). Clear-water scour development at bridge abutments. *Journal of Hydraulic Research*, 41(5), 521–531. doi:10.1080/00221680309499997

Dorosti, M., Bajestan, M. S., & Maymani, F. A. (2018). The effect of slot's distance of triangular spur dike's nose on the pattern of erosion and sediment. *Journal of Water and Soil Science*, 22(2), 67–72. doi:10.29252/jstnar.22.2.67

Emamgholizadeh, S., Nazeri, A., & Azhdary, K. (2021). The effect of different spur dike shapes on bridge abutment scour in compound channel. *Iranian Journal of Irrigation & Drainage*, 15(1), 211–222. https://dorl.net/dor/20.1001.1.20087942.1400.15.1.18.8

Farzin, S., Karami, H., Fazlollahnejad, M., & Nayyer, S. (2018). Numerical modeling and analysis of flow hydrodynamics in flip bucket and approach channel. *Iranian Journal of Watershed Management Science and Engineering*, 12(41), 41–50. http://dorl.net/dor/20.1001.1.20089554.1397.12.41.4.3

Flow Science, I. (2008). FLOW 3D User Manual.

Gu, Z., Cao, X., Jiao, Y., & Lu, W. Z. (2016). Appropriate CFD models for simulating flow around spur dike group along urban riverways. *Water Resources Management*, 30(13), 4559–4570. doi:10.1007/s11269-016-1436-1

Haider, R., Qiao, D., Yan, J., Ning, D., Pasha, G. A., & Iqbal, S. (2022). Flow characteristics around permeable spur dike with different staggered pores at varying angles. *Arabian Journal for Science and Engineering*, 47(4), 5219–5236. doi:10.1007/s13369-021-06435-4

Hasanpour, N., Abdollahpour, M., Khosravinia, P., & Hosseinzadeh Dalir, A. (2012). Effect of slot on time development around the abutments. 9th International River Engineering Conference Shahid Chamran university, 22-24 Jan, 2012, Ahwaz.

Hirt, C. W., & Nichols, B. D. (1981). Volume of fluid (VOF) method for the dynamics of free boundaries. *Journal of computational physics*, 39(1), 201–225. doi:10.1016/0021-9991(81)90145-5

Iqbal, S., Pasha, G. A., Ghani, U., Ullah, M. K., & Ahmed, A. (2021). Flow dynamics around permeable spur dike in a rectangular channel. *Arabian Journal for Science and Engineering*, 46(5), 4999–5011. doi:10.1007/s13369-020-05205-y

Kafle, M. R. (2021). Numerical simulation of meandering effects on velocity field and separation zone past a spur dike in rigid bed. *Nepal Journal of Civil Engineering*, 1(1), 33–40. doi:10.3126/njce.v1i1.43371

Kumar, V. (1996). *Reduction of scour around bridge piers using protection devices*. University of Roorkee.

Kumar, V., Raju, K. G. R., & Vittal, N. (1999). Reduction of local scour around bridge piers using slots and collars. *Journal of hydraulic engineering*, 125(12), 1302–1305. doi:10.1061/(ASCE)0733-9429(1999)125:12(1302)

Masjedi, A., & Jafari, B. (2018). An Iinvestigation into the effect of slot in spur dike on the development of scouring around it in a 180-degree bend. *JWSS-Isfahan University of Technology*, 22(3), 357–371. doi:10.29252/jstnar.22.3.357

Monjezi, A., Masjedi, A., Purmohammadi, M. H., & Heidarnejad, M. (2019). Experimental study of slot effect on the riprap stability around spur dike in river bend. *Iranian Journal of Irrigation &*

Drainage, *13*(3), 627–637. https://idj.iaid.ir/article_95429.html?lang=en

Nayyer, S., Farzin, S., Karami, H., & Rostami, M. (2018). Experimental study on the effect of spur dike's different shapes and on time variation of scour depth around them. *Irrigation and Drainage Structures Engineering Research*, *19*(72), 33–50. doi:10.22092/idser.2017.114741.1238

Nayyer, S., Farzin, S., Karami, H., & Rostami, M. (2019). A numerical and experimental investigation of the effects of combination of spur dikes in series on a flow field. *Journal of the Brazilian Society of Mechanical Sciences and Engineering*, *41*(6), 1–11. doi:10.1007/s40430-019-1757-0

Özyaman, C., Yerdelen, C., Eris, E., & Daneshfaraz, R. (2022). Experimental investigation of scouring around a single spur under clear water conditions. *Water Supply*, *22*(3), 3484–3497. doi:10.2166/ws.2021.389

Pandey, M., Lam, W. H., Cui, Y., Khan, M. A., Singh, U. K., & Ahmad, Z. (2019). Scour around spur dike in sand–gravel mixture bed. *Water*, *11*(7), 1417. doi:10.3390/w11071417

Pandey, M., Valyrakis, M., Qi, M., Sharma, A., & Lodhi, A. S. (2021). Experimental assessment and prediction of temporal scour depth around a spur dike. *International Journal of Sediment Research*, *36*(1), 17–28. doi:10.1016/j.ijsrc.2020.03.015

Tafarojnoruz, A., Gaudio, R., & Calomino, F. (2012). Evaluation of flow-altering countermeasures against bridge pier scour. *Journal of hydraulic engineering*, *138*(3), 297–305. doi:10.1061/(ASCE)HY.1943-7900.0000512

Tripathi, R. P., & Pandey, K. K. (2021). Experimental study of local scour around T-shaped spur dike in a meandering channel. *Water Supply*, *21*(2), 542–552. doi:10.2166/ws.2020.331

Vaghefi, M., Solati, S., & Abdi Chooplou, C. (2021). The effect of upstream T-shaped spur dike on reducing the amount of scouring around downstream bridge pier located at a 180° sharp bend. *International Journal of River Basin Management*, *19*(3), 307–318. doi:10.1080/15715124.2020.1776306